Published in final edited form as:

Brain Res. 2017 February 15; 1657: 297–303. doi:10.1016/j.brainres.2016.12.026.

Effects of VPAC1 activation in nucleus ambiguus neurons

Florin Liviu Gherghina[1,*], **Andrei Adrian Tica**[1,*], **Elena Deliu**[2,#], **Mary E Abood**[2,3], **G. Cristina Brailoiu**[4], and **Eugen Brailoiu**[2,**]

[1]Department of Pharmacology, University of Medicine and Pharmacy, Craiova, Romania, UE

[2]Center for Substance Abuse Research, Temple University School of Medicine, Philadelphia, PA 19140, U.S.A

[3]Department of Anatomy and Cell Biology, Temple University School of Medicine, Philadelphia, PA 19140, U.S.A

[4]Department of Pharmaceutical Sciences, Thomas Jefferson University, Jefferson College of Pharmacy, Philadelphia, PA 19107, U.S.A

Abstract

The pituitary adenylyl cyclase-activating polypeptide (PACAP) and its G protein-coupled receptors, PAC1, VPAC1 and VPAC2 form a system involved in a variety of biological processes. Although some sympathetic stimulatory effects of this system have been reported, its central cardiovascular regulatory properties are poorly characterized. VPAC1 receptors are expressed in the nucleus ambiguus (nAmb), a key center controlling cardiac parasympathetic tone. In this study, we report that selective VPAC1 activation in rhodamine-labeled cardiac vagal preganglionic neurons of the rat nAmb produces inositol 1,4,5-trisphosphate receptor-mediated Ca^{2+} mobilization, membrane depolarization and activation of P/Q-type Ca^{2+} channels. *In vivo*, this pathway converges onto transient reduction in heart rate of conscious rats. Therefore we demonstrate a VPAC1-dependent mechanism in the central parasympathetic regulation of the heart rate, adding to the complexity of PACAP-mediated cardiovascular modulation.

Keywords

autonomic cardiac tone; bradycardia; calcium signaling; PACAP

**To whom correspondence should be addressed: Eugen Brailoiu, M.D., Center for Substance Abuse Research, Temple University School of Medicine, 3500 N. Broad Street, Room 848, Philadelphia, PA 19140, Tel: 215-707-2791, Fax: 215-707-9890, ebrailou@temple.edu.

*Equal Contribution

#Present address: Institute of Science and Technology Austria, Am Campus 1, Klosterneuburg, A-3400, Austria

Conflict of interest statement All authors declare that there are no conflicts of interest.

1. INTRODUCTION

The pituitary adenylyl cyclase-activating polypeptide (PACAP) is a 38-amino acid pleiotropic neuropeptide that belongs to a large superfamily of peptides along with vasoactive intestinal polypeptide (VIP), glucagon, growth hormone-releasing hormone and secretin (Sherwood et al., 2000). PACAP signals via three types of receptors: namely PAC1 receptor, that is PACAP-specific, and VPAC1 and VPAC2 receptors, that have similar affinity for PACAP and VIP (Vaudry et al., 2009). The main signaling mechanism is through Gs proteins, activation of adenyl cyclase and consequent cAMP production (Couvineau and Laburthe, 2012). However, other transduction mechanisms such as Gq coupling and activation of phospholipase C with consequent increase in intracellular calcium levels has been reported in various cell types (Dickson and Finlayson, 2009).

While the PACAP system has been found to play a role in virtually every biological process, its effects on cardiovascular regulation are incompletely characterized (Farnham and Pilowsky, 2010). Peripheral administration of PACAP to cats produces vasodilation at low doses (0.1–0.3 nmol/kg), while at 10 times higher doses the effect is biphasic, comprising of an initial local vasodilatatory effect followed by vasoconstriction (Minkes et al., 1992). However, in dogs, similar systemic low doses of PACAP have been correlated only with pressor and tachycardic responses (Runcie et al., 1995).

The effect of central PACAP administration is, generally, associated with sympathoexcitation. Pressor effects were reported upon PACAP delivery intracerebroventricularly (i.c.v.) to conscious rats (Murase et al., 1993), intracisternally to dogs (Seki et al., 1995) or intrathecally to anesthetized rats (Lai et al., 1997). In another study, PACAP microinjection into the rostral ventrolateral medulla, a key site regulating the sympathetic activity, produced sustained sympathoexcitation and tachycardia along with transient hypertension (Farnham et al., 2012).

Previous studies identified PACAP-like immunoreactivity (Legradi et al., 1994), high levels of VPAC1 and VPAC2 receptor expression, and low to moderate levels of PAC1 receptor immunoreactivity in vagal medullary centers controlling heart rate (Joo et al., 2004). However, the role of the PACAP system in central parasympathetic cardiac regulation has not been characterized. To address this knowledge gap, we investigated the effects mediated by VPAC1 receptor at the level of nucleus ambiguus (nAmb), a critical node governing the cardiac vagal tone (Mendelowitz, 2004).

2. RESULTS

2.1. Activation of VPAC1 increases cytosolic Ca^{2+} concentration in cardiac preganglionic neurons of nAmb

We first examined the effect of [Lys15, Arg16, Leu27]-VIP (1-7)-GRF (8-27)-NH_2 as a selective VPAC1 agonist (Gourlet et al., 1996; Moody et al., 2002) on intracellular Ca^{2+} concentration, $[Ca^{2+}]_i$ and the sensitivity of the response to [Acetyl-His1, D-Phe2, Lys15, Arg16, Leu17] VIP(3-7)/GRF(8-27) or PG97-269, a VPAC1 antagonist (Gourlet et al., 1997). In rhodamine-labeled neurons, the VPAC1 agonist (100 nM) agonist produced a fast

and transient increase in intracellular Ca^{2+} concentration, $[Ca^{2+}]_i$. Pretreatment with the VPAC1 antagonist (10 μM, 20 min) prevented the increase in $[Ca^{2+}]_i$ produced by the VPAC1 agonist. The changes in Fura-2 AM fluorescence ratio upon excitation at 340 and 380 nm are shown in Fig. 1A and the characteristic tracings of $[Ca^{2+}]_i$ changes in Fig. 1B. With increasing concentrations of the VPAC1 agonist (10 nM, 100 nM, and 1000 nM), the effect gradually increased, measuring 127 ± 2.9 nM, 371 ± 3.7 nM and 429 ± 4.1, respectively, at the peak of the response (Fig. 1C). Six cells were examined in each treatment group. Pretreatment with the VPAC1 receptor antagonist reduced the effect of the agonist (100 nM) to insignificant levels of 38 ± 2.4 nM (Fig. 1B, C).

2.2. VPAC1 stimulation in cardiac vagal neurons of nAmb produces Ca^{2+} influx

We next tested the contribution of Ca^{2+} influx and intracellular Ca^{2+} release mechanisms to the elevation in $[Ca^{2+}]_i$ observed upon agonist stimulation of VPAC1 receptors. Inhibition of N-type voltage-gated Ca^{2+} channels (VGCC) with ω-conotoxin GVIA (100 nM, 20 min) had no effect on the Ca^{2+} signal produced by VPAC1 activation in rhodamine-labeled preganglionic neurons (Fig. 2A); the responses measured 371 ± 3.4 nM (n = 6) in the absence versus 362 ± 3.9 nM (n = 6) in the presence of N-type Ca^{2+} channel blocker (Fig. 2B). Pretreatment of neurons with ω-conotoxin MVIIC (100 nM, 20 min), a blocker of P/Q-type of Ca^{2+} channels, significantly blunted the effect of VPAC1 agonist ($\Delta[Ca^{2+}]_i$ was 217 ± 3.6 nM, n = 6, Fig. 2B).

2.3. Activation of VPAC1 releases $Ca^{2+}$from endoplasmic reticulum Ca^{2+} stores

After identification that Ca^{2+} influx via P/Q-type VGCC accounted for only part of the increase in $[Ca^{2+}]_i$ induced by the VPAC1 agonist, we further assessed whether the remaining effect was due to the mobilization of intracellular Ca^{2+} stores. Indeed, in the absence of extracellular Ca^{2+}, VPAC1 activation with 100 nM agonist triggered an increase in $[Ca^{2+}]_i$ by 207 ± 2.3 nM (n = 6) at the peak of the response (Fig. 3A, B); this response is significantly diminished as compared with 371 ± 3.4 nM, when the VPAC1 agonist was administered to neurons incubated in Ca^{2+}-containing saline (Fig 2). Disruption of lysosomal Ca^{2+} stores with bafilomycin A1 (1 μM, 1h pre-incubation), an inhibitor of V-type ATPase that prevents lysosomal acidification, or blocking endoplasmic reticular ryanodine receptors with ryanodine (10 μM, 1h), did not significantly interfere with VPAC1-mediated increase in $[Ca^{2+}]_i$ ($\Delta[Ca^{2+}]_i$ = 201 ± 2.8 nM, and 198 ± 2.6 nM, respectively, 6 neurons tested in each condition). In contrast, in the presence of xestospongin C (10 μM, 15 min) and 2-aminoethoxydiphenyl borate (2-APB, 100 μM, 15 min), which together completely block inositol 1,4,5-trisphosphate (IP_3) receptors (IP_3Rs), the response of rhodamine-labeled cardiac vagal neurons to VPAC1 activation was abolished ($\Delta[Ca^{2+}]_i$ = 38 ± 2.4 nM, n = 6 cells, Fig. 3A, B).

2.4. Depolarizing effect of VPAC1 activation in cardiac vagal neurons of nAmb

The VPAC1 agonist (100 nM) robustly depolarized cardiac-projecting parasympathetic neurons retrogradely labeled with rhodamine; the effect was completely blocked by pretreatment with the VPAC1 antagonist (Fig. 4A). Increasing concentrations of VPAC1 agonist (10 nM, 100 nM, 1000 nM) induced neuronal depolarizations with an amplitude of 2.38 ± 0.7 mV, 7.42 ± 1.6 mV, 9.17 ± 1.8 mV, respectively (Fig. 4B, n = 6 neurons per each

condition), while the effect was basically null with VPAC1 antagonist pretreatment (ΔVm = 0.83 ± 0.4 mV, n = 6, Fig. 4B).

2.5. Microinjection of VPAC1 agonist into the nAmb produces bradycardia in conscious rats

In conscious rats, bearing cannula implanted into the nAmb, microinjection of control saline (50 nL) produced negligible effects on heart rate. Microinjection of L-glutamate (5 mM, 50 nL) elicited bradycardia, without a change in blood pressure (Fig. 5A), indicating the correct placement of the cannula into the nAmb (Brailoiu et al., 2014a; Brailoiu et al., 2013). Two hours after L-glutamate administration, microinjection of VPAC1 agonist (100 nM, 50 nL) promptly and transiently reduced the heart rate (Fig. 5A). No effect on blood pressure was observed. At the concentrations of VPAC1agonist tested here (10 nM, 100 nM and 1000 nM) the heart rate reduction measured 14 ± 1.3 beats per minute (bpm), 37 ± 2.5 bpm and 48 ± 2.7 bpm, respectively (Fig. 5B). Microinjection of the VPAC1 antagonist (500 nM) alone did not elicit a change in heart rate or blood pressure (Fig. 6A). Co-administration of the agonist and antagonist prevented the bradycardia produced by the VPAC1 agonist (100 nM) (Fig. 6A). Comparison of the change in heart rate produced by VPAC1 agonist (100 nM) in the absence and presence of the VPAC1 antagonist, and the lack of effect of the antagonist alone is shown in Fig. 6B. Six animals were used per each treatment group.

3. DISCUSSION

Cardiac-projecting neurons of nAmb plays a critical role in cardiac parasympathetic tone; their activation elicits bradycardia by release of acetylcholine in cardiac ganglia (Dyavanapalli et al., 2016; Mendelowitz, 2004). The activity of nAmb neurons is modulated by G protein-coupled receptors agonists such as nociceptin (Venkatesan et al., 2002; Venkatesan et al., 2003), endomorphin 1 (Irnaten et al., 2003), enkephalin, dynorphin (Wang et al., 2004), orexin A (Dergacheva et al., 2005), isoproterenol and dobutamine (Bateman et al., 2012). We identified several peptides, including urocortin 3 (Brailoiu et al., 2012), nesfatin-1 (Brailoiu et al., 2013b), urotensin II (Brailoiu et al., 2014b), and irisin (Brailoiu et al., 2015), that activate neurons of Amb and produce bradycardia.

In the present study we explored the effects of activation of VPAC1 receptors, which bind PACAP and VIP with similar affinity. Since PACAP also activates PAC1 and VPAC2 receptors, we used a pharmacological approach to examine the effects mediated by VPAC1 receptor in isolation; the selective VPAC1 agonist [Lys15, Arg16, Leu27]-VIP (1-7)-GRF (8-27)-NH_2 (Gourlet et al., 1996; Moody et al., 2002) and the selective VPAC1 antagonist [Acetyl-His1, D-Phe2, Lys15, Arg16, Leu17] VIP(3-7)/GRF(8-27) or PG97-269 (Gourlet et al., 1997). Treatment with the VPAC1 agonist produced a dose-dependent increase in cytosolic Ca^{2+} concentration, $[Ca^{2+}]_{i,}$ in cardiac preganglionic vagal neurons of nAmb retrogradely labeled with rhodamine.

Besides Gs-coupling, VPAC1 activation was also reported to induce Gq-dependent signaling mechanisms and IP_3 receptor-mediated increases in $[Ca^{2+}]_i$ (Dickson and Finlayson, 2009; Jabrane-Ferrat et al., 2000). We identified that in cardiac vagal neurons VPAC1 activation produced Ca^{2+} influx via P/Q-type VGCC, and Ca^{2+} release from endoplasmic reticulum via

IP_3 receptors. Similarly, we found that urocortin 3, via CRF2 receptors in nAmb, increased $[Ca^{2+}]_i$ by releasing Ca^{2+} from endoplasmic reticulum and promoting Ca^{2+} influx through P/Q-type VGCC (Brailoiu et al., 2012). In terms of effects on various types of VGCC, the PACAP system is inhibitory, stimulatory or without effect, depending on the cell system studied and of the type of PACAP receptor involved (Fukushima et al., 2001; Hayashi et al., 2002; Jorgensen et al., 2002; Seebeck et al., 1996; Seebeck et al., 2002). Our present study is the first, to our knowledge, to report VPAC1-mediated activation of the P/Q-type of VGCC. This finding correlates well with the fact that P/Q-channels are the dominant type in cardiac projecting parasympathetic neurons of nucleus ambiguus (Irnaten et al., 2003).

Moreover, we found that stimulation of VPAC1 in cardiac-projecting parasympathetic neurons induces membrane depolarization, which likely triggers activation of the P/Q-type Ca^{2+} channels, providing a correlation between the findings here reported. This cellular pathway converges further to transient reductions in heart rate, an observation in line with our previous reports on other types of systems activating vagal cardiac neurons of nAmb; for instance G-protein coupled estrogen receptor 1-mediated signaling (Brailoiu et al., 2013), nesfatin-1(Brailoiu et al., 2013b) and urotensin II (Brailoiu et al., 2014b).

Interestingly, the PACAP system can also be sympathoexcitatory, both centrally (Farnham et al., 2012) and in the periphery (Runcie et al., 1995). We demonstrate here a potentially counterbalancing effect, translated in parasympathetic-mediated bradycardic responses, via VPAC1 and downstream P/Q VGCC activation in cardiac-projecting nAmb neurons. This hypothesis is supported by the fact that the VPAC1 antagonist, when microinjected alone into nAmb, did not affect the heart rate, indicating that PACAP may not be contribute to the regulation of the basal heart rate, but rather as a compensatory mechanism that may readjust the heart rate. Notably, our findings at the central level are also mirrored in the periphery, since PACAP can induce bradycardia via PAC1 receptors and subsequent N-type VGCC stimulation in atrial cholinergic neurons (Seebeck et al., 1996).

4. EXPERIMENTAL PROCEDURES

4.1. Ethical approval

Animal protocols were approved by the Institutional Animal Care and Use Committee from University of Medicine and Pharmacy Craiova Romania, Thomas Jefferson University and Temple University. All efforts were made to minimize the number of animals used and their suffering.

4.2. Chemicals

All chemicals were from Sigma-Aldrich (St. Louis, MO) unless otherwise mentioned. For all pharmacological studies we used [Lys15, Arg16, Leu27]-VIP (1-7)-GRF (8-27)-NH_2 as a selective VPAC1 agonist (Gourlet et al., 1996; Moody et al., 2002) and [Acetyl-His1, D-Phe2, Lys15, Arg16, Leu17] VIP(3-7)/GRF(8-27) (PG97-269) as a VPAC1 antagonist (Gourlet et al., 1997). In the *in vitro* studies, the antagonist was administered for 10 min before and for the duration of agonist administration; for the *in vivo* studies, the antagonist was loaded in the cannula before the agonist.

4.3. Animals

Neonatal and adult Sprague-Dawley rats (Charles River Laboratories, Wilmington, MA) were used in this study. Neonatal (1–2 days old) rats of either sex were used for retrograde tracing and neuronal culture, and adult male rats (250–300 g) were used for cardiovascular measurements.

4.4. Neuronal labeling and culture

Preganglionic cardiac vagal neurons of nucleus ambiguus were retrogradely labeled by intrapericardial injection of rhodamine [X-rhodamine-5-(and-6)-isothiocyanate; 5(6)-XRITC], 40 μl, 0.01%, (Invitrogen, Carlsbad, CA), as reported (Brailoiu et al., 2014a; Brailoiu et al., 2013). Medullary neurons were dissociated and cultured 24 h after rhodamine injection. In brief, the brains were quickly removed and immersed in ice-cold Hanks' balanced salt solution (HBSS; Mediatech, Manassas, VA). Neonate rats were euthanized by decapitation. The ventral side of the medulla (containing nucleus ambiguus) was dissected, minced, and the cells were subjected to enzymatic and mechanical dissociation. Cells were filtered using a sterile 40 μm filter/cell strainer (Falcon™, Fisher Scientific) and plated on glass coverslips in Neurobasal-A medium (Invitrogen) containing 1% GlutaMax (Invitrogen), 2% antibiotic-antimycotic (Mediatech), and 10% fetal bovine serum. Cultures were maintained at 37 °C in a humidified atmosphere with 5% CO_2. Cytosine β-arabino furanoside (1 μM) was added to the culture to inhibit glial cell proliferation.

4.5. Calcium imaging

Measurements of intracellular Ca^{2+} concentration, $[Ca^{2+}]_i$ were performed as previously described (Brailoiu et al., 2014a; Brailoiu et al., 2013). Briefly, cells were incubated with 5 μM Fura-2 AM (Invitrogen) in HBSS at room temperature for 45 min, and washed with dye-free HBSS. Coverslips were mounted in an open bath chamber (RP-40LP, Warner Instruments, Hamden, CT) on the stage of an inverted microscope Nikon Eclipse TiE (Nikon Inc., Melville, NY), equipped with a Perfect Focus System and a Photometrics CoolSnap HQ2 CCD camera (Photometrics, Tucson, AZ). During the experiments the Perfect Focus System was activated. Fura-2 AM fluorescence (emission 510 nm), following alternate excitation at 340 and 380 nm, was acquired at a frequency of 0.25 Hz. Images were acquired/analyzed using NIS-Elements AR 3.1 software (Nikon). After appropriate calibration with ionomycin and $CaCl_2$, and Ca^{2+} free and EGTA, respectively, the ratio of the fluorescence signals (340/380 nm) was converted to Ca^{2+} concentrations (Grynkiewicz et al., 1985).

4.6. Measurement of membrane potential

The relative changes of neuronal membrane potential were evaluated using bis-(1,3-dibutylbarbituric acid)-trimethine-oxonol, $DiBAC_4(3)$, a voltage-sensitive dye, as reported (Brailoiu et al., 2014a; Brailoiu et al., 2013). Neurons were incubated for 30 min in HBSS containing 0.5 mM $DiBAC_4(3)$ and the fluorescence monitored at 0.17 Hz (excitation/emission 480nm/540nm). Calibration of $DiBAC_4(3)$ fluorescence was performed using the Na^+-K^+ ionophore gramicidin in Na^+-free physiological solution and various concentrations of K^+ and N-methylglucamine.

4.7. Surgical procedures

Adult male Sprague Dawley rats were anesthetized with a mixture of ketamine hydrochloride (100–150 mg/kg) and acepromazine maleate (0.2 mg/kg) as reported (Brailoiu et al., 2014a; Brailoiu et al., 2013). Animals were placed into a stereotaxic instrument; a guide C315G cannula (PlasticsOne, Roanoke, VA) was bilaterally inserted into the nAmb. The stereotaxic coordinates for identification of nAmb were: 12.24 mm posterior to bregma, 2.1 mm from midline and 8.2 mm ventral to the dura mater. A C315DC cannula dummy (PlasticsOne) was used to prevent contamination.

4.8. Non-invasive blood pressure measurement

In rats with cannula inserted into the nAmb, blood pressure was non-invasively measured using a volume pressure recording sensor and an occlusion tail-cuff (CODA System, Kent Scientific, Torrington, CT), as described. One week after the insertion of the cannula, rats were exposed to handling and training every day for 1 week. The maximum occlusion pressure was 200 mm Hg, minimum pressure 30 mm Hg and deflation time 10 s. Two measurements were done per 30 s (one cycle), and the average was used to calculate heart rate, systolic, diastolic and mean arterial blood pressure. Ten acclimatization cycles were done before starting the experiments.

4.9. Microinjection into nAmb

Bilateral microinjections into the nAmb were carried out using the C315I internal cannula (33 gauge, PlasticsOne) and a Neuros Hamilton syringe, without animal handling. Trained rats were in the animal holder for the duration of the experiment. For recovery, at least two hours were allowed between two injections. Injection of L-glutamate (5 mM, 50 nL) was used for the functional identification of nAmb (Brailoiu et al., 2014a; Brailoiu et al., 2013).

4.10. Statistical analysis

Data were expressed as mean ± standard error of mean. Normal distribution of data was examined using Shapiro-Wilk test in Origin 7 (Origin Lab Corporation, Northampton, MA). Samples with normal distribution were further compared for statistically significant differences using one-way ANOVA followed by *post hoc* Bonferroni test, while groups with non-normal distribution were analyzed using the nonparametric Mann-Whitney U test; $P < 0.05$ was considered statistically significant.

Acknowledgments

This study was supported by startup funds from the Jefferson College of Pharmacy, and by the National Institutes of Health DA023204 (to M.E.A) and P30 DA 013429 to Center for Substance Abuse Research, Temple University.

Abbreviations

$[Ca^{2+}]_i$	cytosolic Ca^{2+} concentration
HBSS	Hanks' balanced salt solution
IP_3	inositol 1,4,5-trisphosphate

nAmb	nucleus ambiguus
PACAP	pituitary adenylyl cyclase-activating polypeptide
VIP	vasoactive intestinal polypeptide

References

Bateman RJ, Boychuk CR, Philbin KE, Mendelowitz D. beta adrenergic receptor modulation of neurotransmission to cardiac vagal neurons in the nucleus ambiguus. Neuroscience. 2012; 210:58–66. [PubMed: 22425752]

Brailoiu E, Deliu E, Sporici RA, Benamar K, Brailoiu GC. HIV-1-Tat excites cardiac parasympathetic neurons of nucleus ambiguus and triggers prolonged bradycardia in conscious rats. Am J Physiol Regul Integr Comp Physiol. 2014a; 306:R814–22. [PubMed: 24694382]

Brailoiu E, Deliu E, Sporici RA, Brailoiu GC. Irisin evokes bradycardia by activating cardiac-projecting neurons of nucleus ambiguus. Physiol Rep. 2015:3.

Brailoiu GC, Deliu E, Tica AA, Chitravanshi VC, Brailoiu E. Urocortin 3 elevates cytosolic calcium in nucleus ambiguus neurons. J Neurochem. 2012; 122:1129–36. [PubMed: 22774996]

Brailoiu GC, Benamar K, Arterburn JB, Gao E, Rabinowitz JE, Koch WJ, Brailoiu E. Aldosterone increases cardiac vagal tone via G protein-coupled oestrogen receptor activation. J Physiol. 2013; 591:4223–35. [PubMed: 23878371]

Brailoiu GC, Deliu E, Tica AA, Rabinowitz JE, Tilley DG, Benamar K, Koch WJ, Brailoiu E. Nesfatin-1 activates cardiac vagal neurons of nucleus ambiguus and elicits bradycardia in conscious rats. J Neurochem. 2013b; 126:739–48. [PubMed: 23795642]

Brailoiu GC, Deliu E, Rabinowitz JE, Tilley DG, Koch WJ, Brailoiu E. Urotensin II promotes vagal-mediated bradycardia by activating cardiac-projecting parasympathetic neurons of nucleus ambiguus. J Neurochem. 2014b; 129:628–36. [PubMed: 24521102]

Couvineau A, Laburthe M. VPAC receptors: structure, molecular pharmacology and interaction with accessory proteins. Br J Pharmacol. 2012; 166:42–50. [PubMed: 21951273]

Dergacheva O, Wang X, Huang ZG, Bouairi E, Stephens C, Gorini C, Mendelowitz D. Hypocretin-1 (orexin-A) facilitates inhibitory and diminishes excitatory synaptic pathways to cardiac vagal neurons in the nucleus ambiguus. J Pharmacol Exp Ther. 2005; 314:1322–7. [PubMed: 15947034]

Dickson L, Finlayson K. VPAC and PAC receptors: From ligands to function. Pharmacol Ther. 2009; 121:294–316. [PubMed: 19109992]

Dyavanapalli J, Dergacheva O, Wang X, Mendelowitz D. Parasympathetic Vagal Control of Cardiac Function. Curr Hypertens Rep. 2016; 18:22. [PubMed: 26849575]

Farnham MM, Pilowsky PM. The role of PACAP in central cardiorespiratory regulation. Respir Physiol Neurobiol. 2010; 174:65–75. [PubMed: 20470908]

Farnham MM, Lung MS, Tallapragada VJ, Pilowsky PM. PACAP causes PAC1/VPAC2 receptor mediated hypertension and sympathoexcitation in normal and hypertensive rats. Am J Physiol Heart Circ Physiol. 2012; 303:H910–7. [PubMed: 22886412]

Fukushima Y, Nagayama T, Kawashima H, Hikichi H, Yoshida M, Suzuki-Kusaba M, Hisa H, Kimura T, Satoh S. Role of calcium channels and adenylate cyclase in the PACAP-induced adrenal catecholamine secretion. Am J Physiol Regul Integr Comp Physiol. 2001; 281:R495–501. [PubMed: 11448853]

Gourlet P, Vandermeers A, Vandermeers-Piret MC, Rathe J, De Neef P, Robberecht P. C-terminally shortened pituitary adenylate cyclase-activating peptides (PACAP) discriminate PACAP I, PACAP II-VIP1 and PACAP II-VIP2 recombinant receptors. Regul Pept. 1996; 62:125–30. [PubMed: 8795075]

Gourlet P, De Neef P, Cnudde J, Waelbroeck M, Robberecht P. In vitro properties of a high affinity selective antagonist of the VIP1 receptor. Peptides. 1997; 18:1555–60. [PubMed: 9437716]

Grynkiewicz G, Poenie M, Tsien RY. A new generation of Ca2+ indicators with greatly improved fluorescence properties. J Biol Chem. 1985; 260:3440–50. [PubMed: 3838314]

Hayashi K, Endoh T, Shibukawa Y, Yamamoto T, Suzuki T. VIP and PACAP inhibit L-, N- and P/Q-type Ca2+ channels of parasympathetic neurons in a voltage independent manner. Bull Tokyo Dent Coll. 2002; 43:31–9. [PubMed: 12013823]

Irnaten M, Aicher SA, Wang J, Venkatesan P, Evans C, Baxi S, Mendelowitz D. Mu-opioid receptors are located postsynaptically and endomorphin-1 inhibits voltage-gated calcium currents in premotor cardiac parasympathetic neurons in the rat nucleus ambiguus. Neuroscience. 2003; 116:573–82. [PubMed: 12559112]

Jabrane-Ferrat N, Pollock AS, Goetzl EJ. Inhibition of expression of the type I G protein-coupled receptor for vasoactive intestinal peptide (VPAC1) by hammerhead ribozymes. Biochemistry. 2000; 39:9771–7. [PubMed: 10933794]

Joo KM, Chung YH, Kim MK, Nam RH, Lee BL, Lee KH, Cha CI. Distribution of vasoactive intestinal peptide and pituitary adenylate cyclase-activating polypeptide receptors (VPAC1, VPAC2, and PAC1 receptor) in the rat brain. J Comp Neurol. 2004; 476:388–413. [PubMed: 15282712]

Jorgensen MS, Liu J, Adams JM, Titlow WB, Jackson BA. Inhibition of voltage-gated Ca(2+) current by PACAP in rat adrenal chromaffin cells. Regul Pept. 2002; 103:59–65. [PubMed: 11738249]

Lai CC, Wu SY, Lin HH, Dun NJ. Excitatory action of pituitary adenylate cyclase activating polypeptide on rat sympathetic preganglionic neurons in vivo and in vitro. Brain Res. 1997; 748:189–94. [PubMed: 9067461]

Legradi G, Shioda S, Arimura A. Pituitary adenylate cyclase-activating polypeptide-like immunoreactivity in autonomic regulatory areas of the rat medulla oblongata. Neurosci Lett. 1994; 176:193–6. [PubMed: 7830945]

Mendelowitz, D. Brainstem premotor cardiac vagal neurons. In: Dun, NJ.Machado, BH., Paul, M., editors. Neural Mechanisms of Cardiovascular Regulation. Kluwer Academic Publishers; 2004. p. 371-397.

Minkes RK, McMahon TJ, Higuera TR, Murphy WA, Coy DH, Kadowitz PJ. Analysis of systemic and pulmonary vascular responses to PACAP and VIP: role of adrenal catecholamines. Am J Physiol. 1992; 263:H1659–69. [PubMed: 1481892]

Moody TW, Jensen RT, Fridkin M, Gozes I. (N-stearyl, norleucine17)VIPhybrid is a broad spectrum vasoactive intestinal peptide receptor antagonist. J Mol Neurosci. 2002; 18:29–35. [PubMed: 11931347]

Murase T, Kondo K, Otake K, Oiso Y. Pituitary adenylate cyclase-activating polypeptide stimulates arginine vasopressin release in conscious rats. Neuroendocrinology. 1993; 57:1092–6. [PubMed: 7901784]

Runcie MJ, Ulman LG, Potter EK. Effects of pituitary adenylate cyclase-activating polypeptide on cardiovascular and respiratory responses in anaesthetised dogs. Regul Pept. 1995; 60:193–200. [PubMed: 8746546]

Seebeck J, Schmidt WE, Kilbinger H, Neumann J, Zimmermann N, Herzig S. PACAP induces bradycardia in guinea-pig heart by stimulation of atrial cholinergic neurones. Naunyn Schmiedebergs Arch Pharmacol. 1996; 354:424–30. [PubMed: 8897444]

Seebeck J, Lowe M, Kruse ML, Schmidt WE, Mehdorn HM, Ziegler A, Hempelmann RG. The vasorelaxant effect of pituitary adenylate cyclase activating polypeptide and vasoactive intestinal polypeptide in isolated rat basilar arteries is partially mediated by activation of nitrergic neurons. Regul Pept. 2002; 107:115–23. [PubMed: 12137973]

Seki Y, Suzuki Y, Baskaya MK, Saito K, Takayasu M, Shibuya M, Sugita K. Central cardiovascular effects induced by intracisternal PACAP in dogs. Am J Physiol. 1995; 269:H135–9. [PubMed: 7631841]

Sherwood NM, Krueckl SL, McRory JE. The origin and function of the pituitary adenylate cyclase-activating polypeptide (PACAP)/glucagon superfamily. Endocr Rev. 2000; 21:619–70. [PubMed: 11133067]

Vaudry D, Falluel-Morel A, Bourgault S, Basille M, Burel D, Wurtz O, Fournier A, Chow BK, Hashimoto H, Galas L, Vaudry H. Pituitary adenylate cyclase-activating polypeptide and its receptors: 20 years after the discovery. Pharmacol Rev. 2009; 61:283–357. [PubMed: 19805477]

Venkatesan P, Wang J, Evans C, Irnaten M, Mendelowitz D. Nociceptin inhibits gamma-aminobutyric acidergic inputs to cardiac parasympathetic neurons in the nucleus ambiguus. J Pharmacol Exp Ther. 2002; 300:78–82. [PubMed: 11752100]

Venkatesan P, Baxi S, Evans C, Neff R, Wang X, Mendelowitz D. Glycinergic inputs to cardiac vagal neurons in the nucleus ambiguus are inhibited by nociceptin and mu-selective opioids. J Neurophysiol. 2003; 90:1581–8. [PubMed: 12761284]

Wang X, Dergacheva O, Griffioen KJ, Huang ZG, Evans C, Gold A, Bouairi E, Mendelowitz D. Action of kappa and Delta opioid agonists on premotor cardiac vagal neurons in the nucleus ambiguus. Neuroscience. 2004; 129:235–41. [PubMed: 15489045]

Highlights

- We examined the effect of VPAC1, a receptor for PACAP on nucleus ambiguus, a key center controlling cardiac parasympathetic tone.
- VPAC1 activation at this level, increases cytosolic Ca^{2+}, produces depolarization *in vitro*, and leads to bradycardia *in vivo.*
- Our results unravel a new functional receptor involved in parasympathetic cardiac regulation.

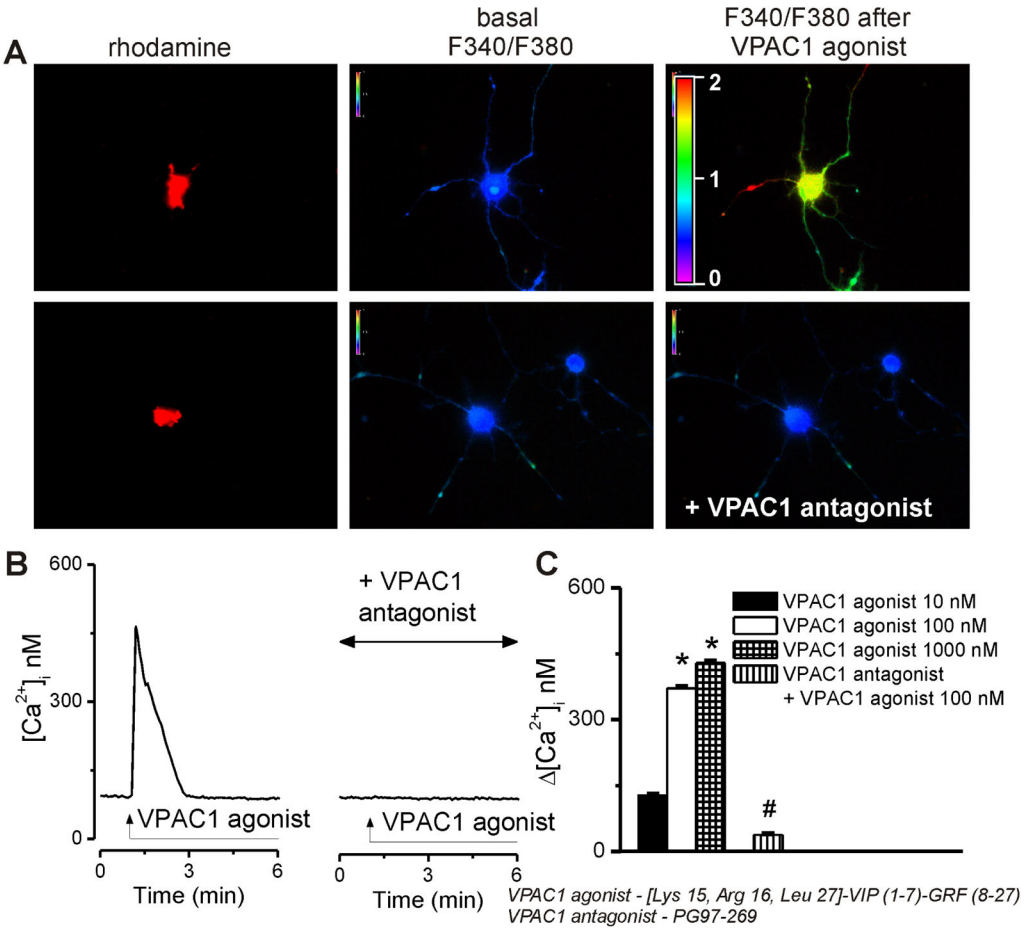

Figure 1. Concentration-dependent $[Ca^{2+}]_i$ elevations induced by VPAC1 activation in cardiac preganglionic vagal nucleus ambiguus neurons

A, Changes in Fura-2 fluorescence ratio (340 nm/380 nm) of rhodamine-labeled neurons upon administration of 100 nM VPAC1 agonist alone (top) and in presence of antagonist pretreatment (bottom). **B,** Typical tracings of Ca^{2+} responses induced by administration of VPAC1 agonist alone (left) or in presence of VPAC1 antagonist. **C,** Concentration-dependent effect of VPAC1 agonist (10–1000 nM) on $[Ca^{2+}]_i$ of cardiac vagal nAmb neurons and lack of effect of 100 nM agonist in neurons pretreated with VPAC1 antagonist (10 μM, 20 min); $^{*}P < 0.05$ compared to basal Ca^{2+} levels and within the group; $^{\#}P < 0.05$ compared to 100 nM agonist.

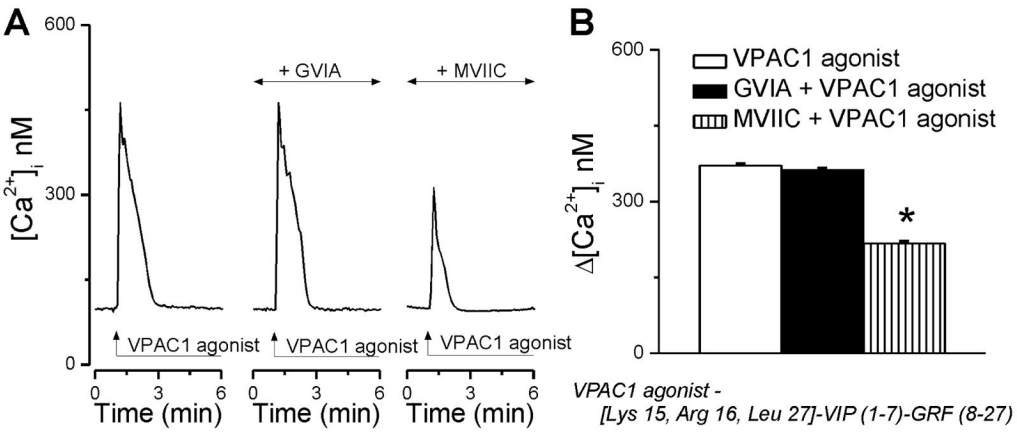

Figure 2. VPAC1 activation triggers Ca^{2+} influx via P/Q-type Ca^{2+} channels

A, Representative examples of Ca^{2+} responses triggered by VPAC1 agonist in the absence and presence of blockers of voltage-activated Ca^{2+} channels (N-type, ω-conotoxin GVIA; P/Q-type, ω-conotoxin MVIIC). **B,** Quantification of the increase in $[Ca^{2+}]_i$ produced by VPAC1 stimulation in the conditions mentioned in A; $*P < 0.05$ compared with VPAC1 agonist alone.

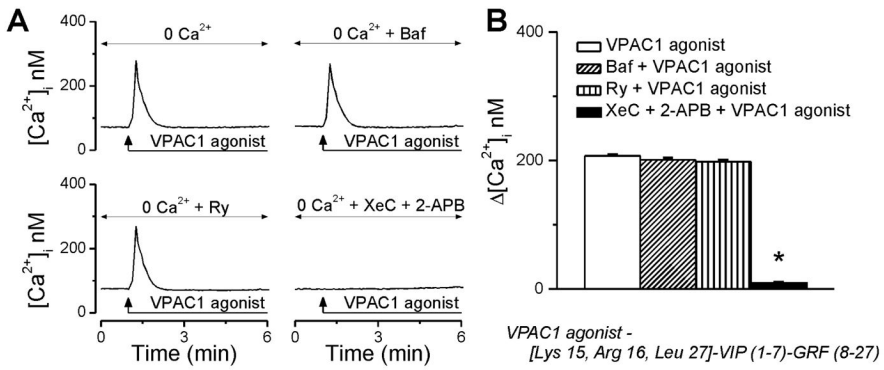

Figure 3. VPAC1 activation releases Ca^{2+} from IP_3-sensitive Ca^{2+} stores in cardiac vagal neurons of nucleus ambiguus

A, Characteristic increases in $[Ca^{2+}]_i$ produced by VPAC1 agonist (100 nM) in Ca^{2+}-free saline, in the absence and presence of lysosomal disruptor bafilomycin A1 (Baf), ryanodine receptor blocker ryanodine (Ry), IP_3R inhibitors xestospongin C (XeC) and 2-aminoethoxydiphenyl borate (2-APB). **B,** Comparison of the effects on $[Ca^{2+}]_i$ induced by treatments indicated in A, in cultured cardiac vagal neurons; $*P < 0.05$ as compared with VPAC1 agonist alone.

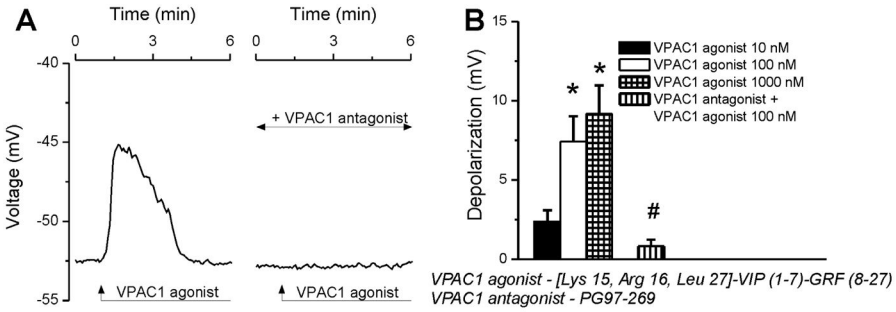

Figure 4. VPAC1 activation depolarizes cardiac vagal neurons of nucleus ambiguus

A, Representative changes in membrane potential elicited by VPAC1 agonist (100 nM) alone or after antagonist (10 μM) pretreatment in rhodamine-labeled cardiac vagal nAmb neurons. **B,** Response quantifications reveal concentration-dependent depolarizing effect of VPAC1 agonist (10–1000 nM) on the membrane potential of cardiac preganglionic neurons; $^{*}P < 0.05$ compared with resting membrane potential and within the group, $^{\#}P < 0.05$ compared to the effect of 100 nM VPAC1 agonist.

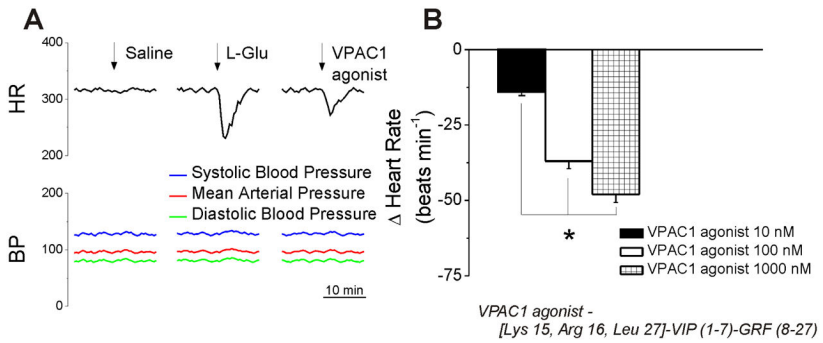

Figure 5. Bradycardic effects of microinjection of VPAC1 agonist in the nucleus ambiguus of conscious rats

A, Characteristic heart rate and blood pressure recordings after microinjection of saline, L-glutamate (L-Glu, 5 mM, 50 nL) and VPAC1 agonist (100 nM, 50 nL). **B,** Microinjection of VPAC1 agonist (10, 100 and 1000 nM) induces dose-dependent bradycardic responses. **P* < 0.05 as compared to basal heart rate and within the group.

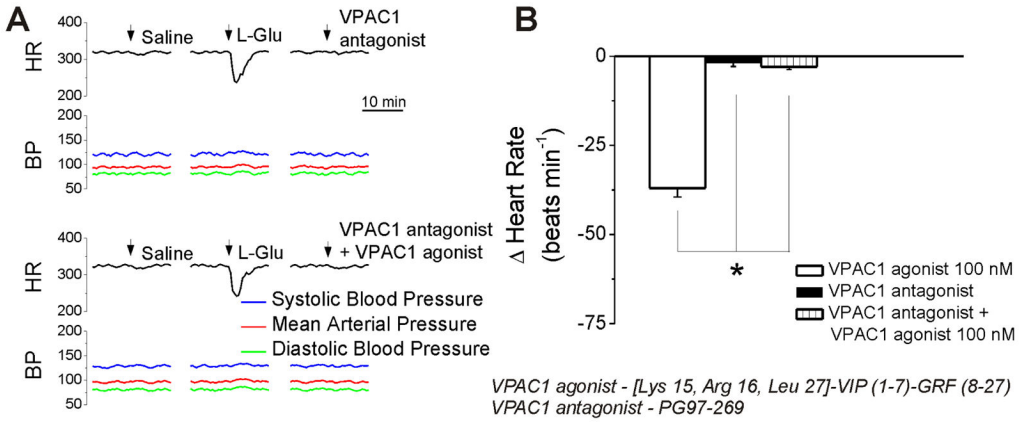

Figure 6. Microinjection of VPAC1 antagonist into the nucleus ambiguus prevents the bradycardic effect of the VPAC1 agonist in conscious rats

A, Representative examples of heart rate and blood pressure recordings after microinjection of saline, L-glutamate (L-Glu, 5 mM, 50 nL), VPAC1 antagonist (500 nM, 50 nL) alone, and co-administration of VPAC1 antagonist (500 nM, 50 nL) and VPAC1 agonist (100 nM, 50 nL). The bradycardic effect of VPAC1 agonist (100 nM) is blocked by co-administration of VPAC1 antagonist; $*P < 0.05$ compared with the effect of the antagonist alone or of the co-administration of the antagonist and agonist.

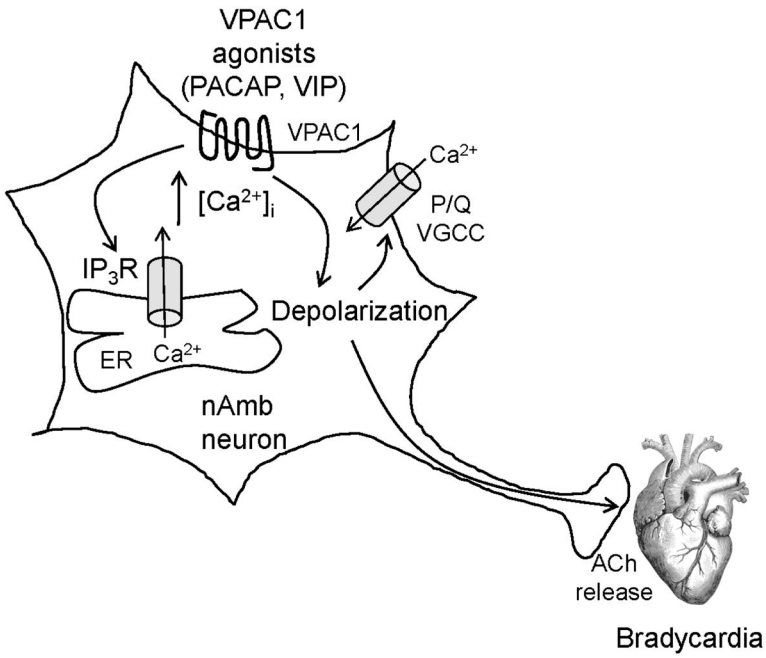

Figure 7. Diagram summarizing the effects of VPAC1 receptor activation in the nucleus ambiguus neurons

VPAC1 agonists such as PACAP or VIP activate VPAC1 receptor and release Ca^{2+} from endoplasmic reticulum (ER) via inositol 1,4,5-trisphosphate receptor (IP_3R). VPAC1 agonists also produce membrane depolarization, facilitating activation of P/Q-type voltage-gated Ca^{2+} channels (VGCC) and subsequent Ca^{2+} influx. The depolarization is transmitted along the axon and leads to the release of acetylcholine (ACh) in cardiac ganglia followed by bradycardia.